

Multidisciplinary Framework for the Conceptual Analysis of Asteroid Capture Missions

Manuel A. Tejeira* and Akira Jinkoji†

Georgia Institute of Technology, Atlanta, GA, 30332, USA

Yani Ait Ammar‡, Zachary Brinsfield§, and Salma Benhissoune¶

Georgia Institute of Technology, Atlanta, GA, 30332, USA

Sonal Mehta|| and Jeremiah D. Jensen**

Georgia Institute of Technology, Atlanta, GA, 30332, USA

Tristan Sarton du Jonchay†† and Dimitri N. Mavris‡‡

Georgia Institute of Technology, Atlanta, GA, 30332, USA

Near-Earth Asteroids have attracted consistent interest for the important insights they provide about the early solar system and human origins, their potential for commercial use, and the relevance to spot and prevent possible impact threats to Earth. Designing asteroid capture missions, however, is a complex and costly process requiring evaluation of asteroid reachability, mission alignment, and uncertainties in key parameters, all of which impact mission planning and spacecraft design. To address these challenges, this study presents an integrated parametric tool for early-phase design and assessment of asteroid capture missions. The tool is built around a multidisciplinary modeling and simulation framework that unifies trajectory analysis, rendezvous and proximity operations, and subsystem-level spacecraft sizing. A design of experiments approach is used to generate training data, from which surrogate models are built to enable rapid trade space exploration. An interactive dashboard allows users to assess mission feasibility, explore trade-offs between key parameters, and visualize mission timelines and subsystem breakdowns. Case studies on two near-Earth asteroids, 2008 EA9 and 2009 BD, demonstrate the tool's ability to identify feasible mission regions and evaluate sensitivity to asteroid uncertainties and launch conditions, supporting informed decision-making in the conceptual design phase.

I. Nomenclature

ΔV	= Change in Velocity
I_{sp}	= Specific Impulse
TOF	= Time of Flight
m_{in}	= Input Gross Mass Value of the Spacecraft for the Trajectory Model
m_{req}	= Required Gross Mass of the Spacecraft for the Mission
m_p	= Propellant Mass Consumed
m_{max}	= Maximum Payload Mass of Launch Vehicle

*Graduate Research Assistant, Aerospace System Design Laboratory (ASDL), School of Aerospace Engineering, AIAA Student Member.

†Graduate Research Assistant, ASDL, School of Aerospace Engineering, AIAA Student Member.

‡Graduate Research Assistant, ASDL, School of Aerospace Engineering.

§Graduate Student, ASDL, School of Aerospace Engineering. The views expressed in this article are those of the author and do not reflect the official policy or position of the Department of the Air Force, Department of Defense, or the U.S. Government.

¶Graduate Research Assistant, ASDL, School of Aerospace Engineering.

||Graduate Research Assistant, ASDL, School of Aerospace Engineering, AIAA Student Member.

**Graduate Research Assistant, ASDL, School of Aerospace Engineering, AIAA Student Member.

††Research Engineer II, ASDL, School of Aerospace Engineering, AIAA Member.

‡‡Georgia Tech Distinguished Regents Professor and Director of ASDL, AIAA Fellow

II. Introduction

ASTEROID capture missions represent a growing subject of strategic space endeavors focused on the advancement of human space exploration. These missions aim to rendezvous and potentially redirect small celestial bodies, fulfilling several critical objectives. First, they contribute directly to planetary defense by enabling the controlled study and deflection of potentially hazardous near-Earth objects (NEOs). Second, they serve as platforms for scientific discovery, offering access to primitive material from the early solar system. Finally, they unlock the possibility of commercial utilization of space resources, laying the foundation for in-space economies based on asteroid mining.

The importance of planetary defense has become more urgent as our ability to detect and catalog NEOs improves. One example is the Apophis asteroid, which drew widespread attention when early observations indicated a potential impact in 2029 [1]. Although refined tracking has ruled out this scenario, Apophis remains a symbolic threat posed by near-Earth asteroids (NEAs). According to the Jet Propulsion Laboratory (JPL) of NASA, NEOs are continually monitored for Earth impact probability, some of which exceed 1 kilometer in diameter [2]. An Earth collision with such a body would result in global-scale devastation. Therefore, asteroid capture missions are an invaluable investment towards enabling planetary protection.

Scientifically, asteroids are time capsules of the early solar system, preserving material that has remained largely unchanged since planetary formation [3]. By studying asteroid composition, scientists can gain valuable insight into how planets and other celestial bodies began to form and grow. Missions like Origins, Spectral Interpretation, Resource Identification, and Security-Regolith Explorer (OSIRIS-REx) have shown that asteroid surfaces can differ significantly from telescope observations, revealing unexpected regolith compositions [4]. By capturing and returning an asteroid, researchers can directly compare observational models with actual data, improving asteroid classification methods for future exploration and planetary defense efforts.

The commercial sector also has a strong interest in asteroid capture missions, particularly due to the economic potential of asteroid mining. Many asteroids contain water, metals, and rare elements that could serve as raw materials for both space-based manufacturing and terrestrial markets [3]. One of the most valuable resources is Helium-3, an isotope that is rare on Earth but abundant in space. For example, ten tons of Helium-3 could supply enough energy to meet Earth's daily power consumption using fusion reactors [3]. Although the technology required for large-scale asteroid mining is not yet mature, asteroid capture missions offer a vital stepping stone for developing in-situ resource utilization (ISRU) infrastructure.

Several missions have already advanced the state of the art in asteroid capture and proximity operations. Japanese Aerospace Exploration Agency's (JAXA) Hayabusa program demonstrated sample return from Itokawa and later Ryugu, validating navigation techniques, surface interaction, and sample collection in low-gravity environments [5]. NASA's OSIRIS-REx mission extended this capability by successfully acquiring and returning samples from asteroid Bennu [6]. In contrast, NASA's Asteroid Redirect Mission (ARM) aimed to capture a small asteroid or a boulder from a larger body and relocate it to lunar orbit [7]. Though ARM was canceled due to shifting political priorities, it highlighted the growing ambition of asteroid capture missions and the significant resources required to accomplish such endeavors.

The planning timelines and costs for these missions have been considerable. Hayabusa 1 took nearly a decade from concept to launch and cost over \$100 million [8] [9]. OSIRIS-REx required more than 5 years of development and a budget approaching \$1 billion [10] [11]. Even ARM, which was never launched, consumed years of planning, engineering studies, and early system integration efforts [12] [13]. These examples underline a central challenge in asteroid mission development: the early design phase, or conceptual study, is resource-intensive and characterized by high uncertainty [14]. Engineers and scientists must consider a wide range of variables, including asteroid size, composition, spin state, and orbit, along with propulsion system design, spacecraft mass, launch timing, and more. This complexity often necessitates iterative studies by large interdisciplinary teams over long periods.

Recent progress in computational modeling and optimization tools offers the potential to reduce this burden. Libraries such as PyKEP allow for trajectory optimization under low-thrust constraints, while frameworks like OpenMDAO support multidisciplinary system design and trade studies. However, most available tools are domain-specific and do not account for the tight coupling between mission trajectory and spacecraft sizing, particularly in asteroid capture scenarios. For example, an asteroid's mass and spin rate directly affect capture strategy, which in turn determines the power and mass required for propulsion and structural subsystems. Traditional mission design methods treat these components in a distributed and sequential manner rather than as part of an integrated system, limiting their effectiveness during the earliest and most uncertain phases of design. According to NASA's mission lifecycle, deep space projects often involve distributed collaboration among multiple NASA centers, universities, and science organizations [14], further emphasizing the need for integrated tools that can coordinate interdependent design decisions across domains.

To address this gap, this paper introduces an integrated modeling and simulation (M&S) framework designed to

support asteroid capture mission planning from concept to system-level design. The framework unifies three primary disciplines: (1) low-thrust trajectory optimization using PyKEP, (2) modeling of rendezvous and proximity operations (RPO), including observation, approach, spin-matching, capture, and detumbling, and (3) spacecraft subsystem sizing based on propulsion needs and mission profile. The tool accepts user-defined inputs such as launch window, maximum *TOF*, propulsion parameters, and asteroid characteristics, and it outputs feasibility assessments, trajectory timelines, and subsystem mass distributions. Through this integration, the tool enables trade space exploration and early identification of viable mission architectures.

Through the study, this work makes several key contributions: (1) the development of a unified simulation environment that integrates trajectory design, RPO, and spacecraft sizing; (2) the implementation of a combined design of experiments (DOE) and surrogate modeling framework that enables users to assess how timeline and asteroid parameters influence mission feasibility and spacecraft mass sensitivity, and to efficiently approximate mission outcomes; (3) the creation of an interactive dashboard interface that allows users to rapidly explore the mission tradespace across multiple asteroid targets and visualize how design parameters impact mission performance. Case studies on two asteroid targets, 2008 EA9 and 2009 BD, are run through this pipeline to illustrate how the tool can reveal feasible mission regions and identify sensitivity trends in spacecraft sizing.

In the following sections, **Section III** presents the methodology, outlining the integration of trajectory design, RPO, and spacecraft sizing into the simulation tool. **Section IV** describes the implementation of the DOE approach and the development of surrogate models to efficiently approximate key metrics, such as mission feasibility and spacecraft mass, across large input spaces. It also includes the application of the tool to two asteroid case studies, 2008 EA9 and 2009 BD, highlighting their impact on spacecraft mass and mission success. Finally, **Section V** concludes with a summary of findings and outlines potential future extensions to the tool.

III. Methodology

This section outlines the technical approach used to address the asteroid capture problem. Largely based on the architecture planned by the NASA ARM [15], the mission timeline is illustrated in the bat chart in Figure 1, providing an overview of the flight sequence.

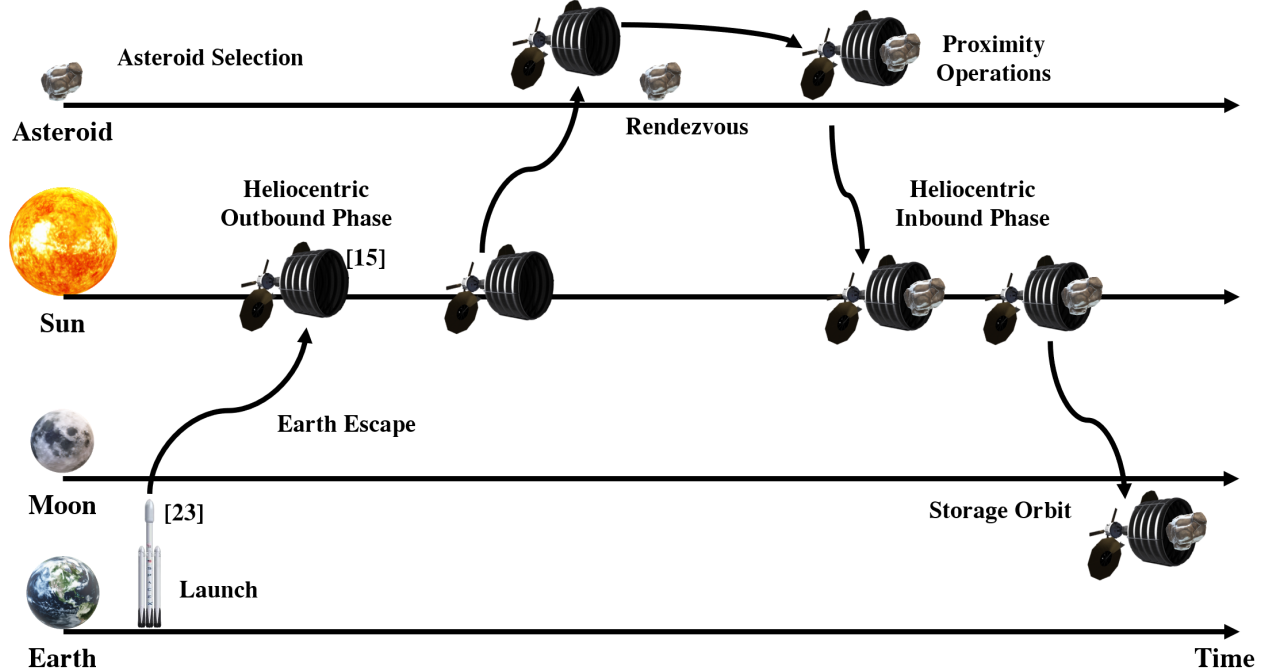


Fig. 1 Asteroid capture mission bat chart

The mission is divided into the following phases:

- **Asteroid Selection:** The target asteroid is selected, and its physical and orbital parameters are retrieved from

available databases.

- **Launch and Earth Escape:** The spacecraft is launched and placed on a trajectory that escapes Earth’s sphere of influence to begin interplanetary travel.
- **Heliocentric Outbound Phase:** The spacecraft travels to the target asteroid.
- **Rendezvous and Proximity Operations:** This phase includes rendezvous, in-situ characterization of the asteroid, approach, and capture operations.
- **Heliocentric Inbound Phase:** After capture, the asteroid is transported back to cislunar space.
- **Storage Orbit:** The spacecraft and asteroid are injected into a stable orbit around the Earth–Moon system to enable future exploration and analysis by crewed missions.

A. Technical Approach

Asteroid capture missions depend on a wide range of factors, including the choice of target asteroid, launch date, mission duration, propulsion system, and capture strategy. This project aims to assess the feasibility of such missions under user-defined constraints: namely, the selected asteroid, launch window, and maximum mission duration. This is achieved through low-thrust trajectory analysis, detailed modeling of RPO phases and the capture system, and spacecraft subsystem sizing. The objective is to enable users to systematically explore the mission design space and assess trade-offs, such as those between mission duration and spacecraft mass. To support this, the approach is divided into the following modeling blocks, which are detailed in the next subsection: trajectory optimization, RPO modeling, and spacecraft subsystem sizing.

The first step is to retrieve relevant asteroid data, including orbital elements, ephemerides, and physical characteristics. Several databases are available for this purpose. NASA JPL’s Small-Body Database provides detailed orbital and physical data on numerous NEAs [16], while the International Astronomical Union Minor Planet Center Orbit Database (MPCORB) also offers ephemerides of several celestial bodies [17]. For smaller asteroids, where some parameters may be missing or uncertain, default values based on scientific estimates or literature approximations are used.

The retrieved asteroid parameters are used by the Trajectory Model to compute the total ΔV and TOF required to reach the asteroid and return it to cislunar space. This model takes as inputs: an initial mass estimate, a specified launch window, and the maximum mission duration. The trajectory model also requires inputs from the RPO Model: the ΔV , TOF , and propellant mass needed for proximity operations and capture.

The capture mechanism is tailored to the selected asteroid’s properties, such as size, diameter, density, and rotation, sourced from the asteroid databases. These factors drive the design and mass of the capture system, which is computed by the RPO model and then passed to the Spacecraft Sizing Model as a fixed mass contribution.

The Spacecraft Sizing Model uses outputs from the Trajectory and RPO Models to estimate the minimum feasible total spacecraft mass. This includes allocating mass across all subsystems, with emphasis on the propulsion system (to meet ΔV requirements), the power system (to support propulsion), and other core subsystems such as communications, avionics, and thermal control.

Each model can then be combined, yielding sized and mass-allocated spacecraft designs and decomposed launch and mission schedules for feasible mission plans. If a mission plan is found to be infeasible, the model will note its infeasibility, allowing for future examination of mission feasibility behavior as a function of the inputs. The full solution process, depicted in Figure 2, presents a detailed activity diagram outlining each step’s inputs, outputs, and data flows.

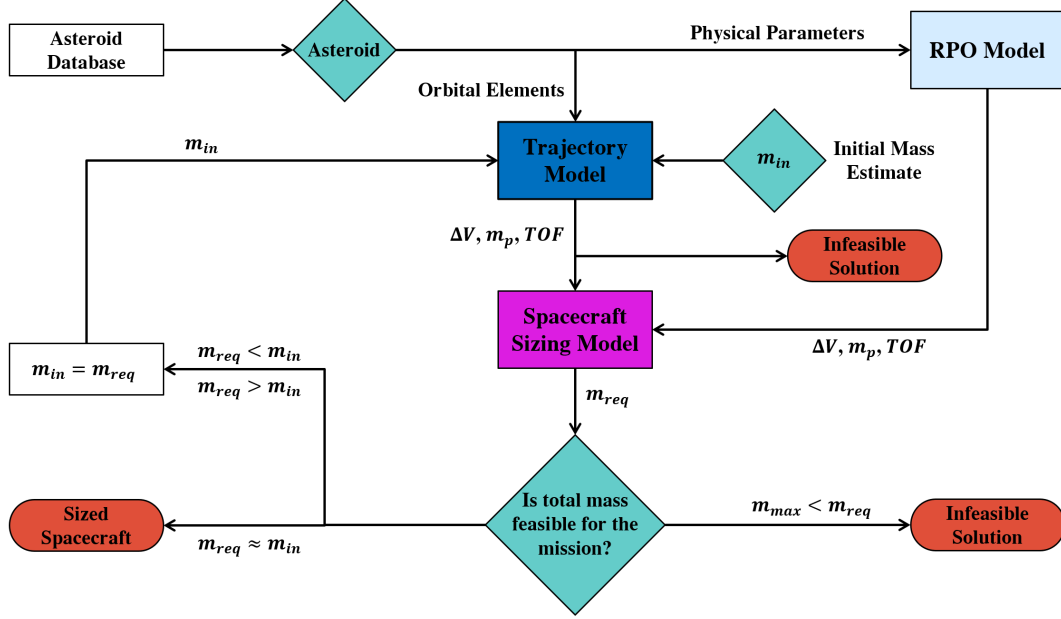


Fig. 2 Technical approach activity diagram

After running the Spacecraft Sizing Model, a decision must be made based on the spacecraft's mass: Is further iteration over spacecraft mass required, or is the design infeasible? If the spacecraft's mass is roughly equivalent to the trajectory model's mass estimate, the spacecraft is considered sized and a feasible solution is obtained. If it is significantly less than the initial mass estimate, the mass is passed back to the trajectory model for further iteration. If the spacecraft mass is greater than the maximum payload mass of the launch vehicle, then the design is considered infeasible. In addition, if the Trajectory Model fails to find a solution where the mission duration is longer than the given mission window, then the design is infeasible. Each model will be discussed in further detail in this section to provide a more thorough understanding of the full technical approach.

B. Trajectory Model

The trajectory model aims to determine the control laws of the thruster that minimize overall propellant consumption for the mission. For each leg or phase, it outputs the ΔV , TOF , and propellant mass required, which are then used by the spacecraft sizing model.

The choice of propulsion system is primarily driven by the high payload capacity required by the mission. Notably, the mass of an asteroid is several orders of magnitude greater than that of the spacecraft. As a result, the dominant sizing parameter for the propulsion system is the ΔV required to return the target asteroid to Earth. This necessitates a highly efficient propulsion system. Solar electric propulsion (SEP) systems offer significantly higher specific impulse (I_{sp}) than conventional chemical engines, resulting in reduced propellant mass and extended operational range [18, 19]. In this study, we adopt the propulsion system envisioned for the NASA ARM [7], consisting of three xenon thrusters with a total power consumption of 42 kW, an efficiency of 57%, and a specific impulse of 3300 s. Note that these values can be parametrically adjusted within the modeling environment to accommodate alternative propulsion system characteristics.

However, low-thrust propulsion introduces key trade-offs. The reduced thrust implies longer mission durations, and low-thrust trajectory analysis introduces additional complexity. Specifically, the problem involves continuous control optimization and numerically ill-conditioned dynamics [20] as the propulsion system must operate over extended durations. Most tools developed by space agencies for this purpose (e.g., NASA's MYSTIC, COPERNICUS, ANSYS STK) are high-fidelity and computationally intensive [21], making them unsuitable for integration into the rapid conceptual design phase of a mission.

To address this, we adopt a simplified trajectory model based on the patched conic approximation. This method segments the overall trajectory into a series of distinct two-body problems [22], where, at each phase, only the gravitational influence of the dominant celestial body is considered. The model is further simplified by relying on the following assumptions. Note that the RPO phase modeling is described in the next subsection.

- **Launch and Earth escape:** Several options exist for the initial Earth departure phase. One method involves placing the spacecraft in a parking orbit and using its low-thrust propulsion system to spiral out of Earth’s gravity well. However, this strategy demands excessive ΔV and long transfer times. Instead, we assume the spacecraft is launched directly onto an escape trajectory by a launch vehicle. This simplifies the analysis by excluding spacecraft propellant use and time during this phase. To generalize across mission targets, we further assume a parabolic escape with a characteristic energy $C_3 = 0$, setting the spacecraft’s initial heliocentric state independently of the asteroid’s orbit. While this neglects early mission dynamics (e.g., gravity assists), it enables a clean boundary condition for heliocentric optimization. A key tradeoff is that the spacecraft mass is constrained by launcher capacity. For example, Space Launch System (SLS) Block 1, SLS Block 1B, and Falcon Heavy can place approximately 25, 40, and 10 metric tons, respectively, on such escape trajectories [23, 24].
- **Heliocentric Outbound and Inbound Phases:** In these two phases, the Sun is the only gravitationally influential body. Using the spacecraft’s low-thrust propulsion system, we aim to determine the departure dates, times of flight, and thrust profiles that minimize round-trip propellant consumption while satisfying key mission constraints, namely the launch window and maximum mission duration. Trajectory optimization is performed using PyKEP [25], a scientific Python library for astrodynamics developed by the European Space Agency (ESA). Among its modules is `1t_margo`, which is specifically designed to solve low-thrust rendezvous problems with NEAs. PyKEP is particularly well-suited for this project’s trajectory model, as it is open-source, computationally efficient - though at the expense of lower fidelity solutions - and implemented in Python, which facilitates integration with the other tools in the modeling framework. The Outbound and Inbound phases are more thoroughly described below:
 - **Earth to Asteroid (Outbound phase):** This phase begins when the spacecraft reaches its parabolic escape trajectory. The initial position and velocity of the spacecraft at the start of the heliocentric outbound phase match those of Earth. The goal is to rendezvous with the asteroid, so the final state matches the asteroid’s position and velocity at the arrival date. A tolerance of 1,500 km is used for the relative position, and 0.3 m/s for the relative velocity, following what was done in [26]. The module’s code is slightly modified by adding a penalty term to the objective function to ensure that all constraints are satisfied and that feasible trajectories are computed. Note that the optimization algorithm is stochastic, so the results depend heavily on the initial guess. Therefore, multiple optimization runs are necessary to identify the best solution.
 - **Asteroid to Earth (Inbound phase):** This phase begins at the end of the RPO phase. Once the asteroid is captured, we assume that the spacecraft can wait for a maximum of one year (stand-by phase) in the asteroid’s orbit, awaiting a suitable departure window back to Earth. We are also solving for a rendezvous problem for this phase: the initial state corresponds to the asteroid’s position and velocity at the departure date, and the final state corresponds to Earth’s position and velocity at the arrival date. Note that for this phase, we must account for the added mass of the asteroid to the spacecraft’s mass. The tolerances on the final state are increased for this phase, as we do not aim to rendezvous precisely with Earth but rather to reach cislunar space. From there, the spacecraft uses lunar gravity assist maneuvers to insert into a stable orbit around the Moon and place the target in a safe storage orbit. A tolerance of 10,000 km is used for the relative position, and 1 km/s for the relative velocity. The same `1t_margo` module is used to calculate the trajectory for this phase, but we adapt it to meet our specific needs.
- **Storage Orbit Phase:** This phase corresponds to the spacecraft’s initial lunar capture upon return to cislunar space, followed by its transition into a stable storage orbit. To enable long-term study of the captured asteroid, this orbit must remain stable over an extended duration. During the planning of the ARM mission, NASA proposed a strategy involving low-thrust arcs, lunar flybys, and small perturbations applied over time to gradually insert the asteroid-laden spacecraft into a relatively stable distant retrograde orbit (DRO) around the Moon [13]. As this phase constitutes a three-body problem, there is no simple analytical method to determine the required propellant mass or *TOF*. To address this, we adopt estimates from the NASA ARM study, which relied on high-fidelity trajectory tools for the asteroid 2009 BD. That study reported a *TOF* of approximately 1.4 years and a total ΔV of 60 m/s [15]. In our model, these values are used to estimate the propellant mass consumption for this segment. The calculation is based on the spacecraft’s mass at the end of the heliocentric inbound phase, using the rocket equation. While this approach is not strictly valid for low-thrust trajectories, it provides a reasonable approximation of the required propellant.

Having defined the models for each trajectory segment, we now focus on optimizing the full trajectory to minimize total propellant consumption while satisfying user-defined constraints on *TOF*, launch window, and spacecraft mass.

The inbound and outbound heliocentric legs are the primary drivers of propellant use, especially the inbound phase due to the added asteroid mass, and are therefore the focus of the optimization for which either of two approaches - Forward or Backward - can be followed:

Forward Optimization Approach. A first, intuitive strategy is to solve the trajectory sequentially: outbound leg first, followed by the inbound leg. The available *TOF* is computed by subtracting fixed durations (e.g., 4 months for RPO, standby time, and storage orbit phase) from the user-specified mission duration. Various *TOF* splits between outbound and inbound legs (e.g., 50/50, 40/60) are tested. The outbound leg is optimized first, and its output defines the start conditions for the inbound leg. However, this approach is sensitive to the inbound departure window: small changes can render the solution infeasible or lead to large increases in propellant needs. In practice, minor savings on the outbound leg can result in disproportionately high costs on the inbound leg.

Backward Optimization Approach. To mitigate this, a second approach reverses the optimization order. For each *TOF* split, the inbound leg is optimized first, using an estimated spacecraft mass (initial mass minus estimated outbound propellant) and a departure window derived from launch and mission constraints. This estimation is justified as the asteroid mass dominates the inbound phase mass budget. For each viable inbound trajectory, a corresponding outbound leg is computed to match arrival conditions and mission constraints. The pair minimizing total propellant consumption is selected. The final trajectory is then reconstructed using the selected outbound leg, the corresponding RPO timeline, and the optimized inbound leg, now with updated spacecraft mass. The propellant for the storage orbit phase is finally added, completing the estimation. This backward approach improves robustness by prioritizing the more propellant-intensive and sensitive inbound phase, leading to more efficient overall mission planning.

C. Rendezvous and Proximity Operations Model

The rendezvous, proximity operations, and capture modeling process focuses on the spacecraft's close approach, capture, and stabilization of the asteroid. This process is structured into six main steps: observation, maneuver to the spin axis, spin rate matching, close approach, capture mechanism deployment, and detumbling.

- **Step 1:** In the observation phase, the spacecraft holds a stand-off position while utilizing sensors and cameras to determine the asteroid's spin axis and rotation rate. Computer vision algorithms analyze captured images to compute these parameters in inertial space. The output of this phase is the time required to determine the spin-axis orientation and spin rate, based on data from Barbee et al.[27].
- **Step 2:** The spacecraft maneuvers from its initial observation point to a predetermined location along the spin axis of the asteroid, positioned 10 meters above the surface. A low-thrust trajectory model, based on the Clohessy-Wiltshire equations, is used to calculate the required thrust input, assuming a circular orbit and negligible asteroid gravity [28]. A Python implementation of this model estimates the total propellant consumed, the duration of the maneuver, and provides a trajectory plot of the spacecraft's path.
- **Step 3:** The spacecraft synchronizes its rotation with the asteroid's spin rate while maintaining the capture system oriented toward the target. The simulation uses a sliding mode control law for attitude tracking to ensure fuel-optimal maneuvers [29]. To simplify the spacecraft's mass properties, a cylindrical geometry with uniform mass distribution is assumed with the capture system aligned along the revolution-axis. Given the high angular momentum requirements (on the order of $10^4 \text{ N}\cdot\text{m}\cdot\text{s}$), monopropellant hydrazine thrusters were selected for attitude control, as reaction wheels cannot provide sufficient torque. Based on a Reaction Control System (RCS) configuration from Pasand et al.[30], the simulation converts the commanded torque into individual thruster commands to estimate propellant mass consumption. Iterative adjustments are applied to ensure that thrust commands remain within operational limits, enabling accurate modeling of fuel usage.
- **Step 4:** The spacecraft performs a close approach to the asteroid. This final maneuver is assumed to require a ΔV of 1.9 m/s and a flight time of approximately 23 minutes, based on data from Barbee et al.[31]. The corresponding propellant mass consumption is then calculated using the Tsiolkovsky rocket equation.
- **Step 5:** This phase involves the deployment of the capture mechanism. A qualitative trade-off analysis was conducted to evaluate various capture system options, including flexible connection systems (e.g., net, harpoon, tether-gripper), stiff connection systems (e.g., robotic arms, tentacles), and NASA's bag capture system. The evaluation criteria considered were target flexibility, post-capture maneuverability, system impact, technology readiness level (TRL), and design complexity. Table 1 summarizes this comparison.

Flexible systems provide adaptability and lower mass but pose collision risks and lack detumbling capabilities.

Table 1 Capture systems trade-offs

Criteria	Flexible (Net/Harpoon/Tether)	Stiff Connection (Robotic Arms/Tentacles)	NASA Bag Capture System
Target Flexibility	Large spin rate and size flexibility[32]	Requires grappling points[33]	Adapts to asteroid surface uncertainties[34]
Post-Capture Maneuverability	Risk of collision, no detumbling capability[35]	Rigid connection enables detumbling [32]	Quasi-rigid via inflatable structure, designed for detumbling [27][34]
System Impact	Lightweight, large capture distance [32]	High mass, close contact required[32][33]	Close contact required, mass estimated at 500–600 kg
TRL	4–7 (harpoon/net)[33]	7 (robotic arms)[33], 4 (tentacles) [33]	5–6 (Estimation based on [27][34])
Cost/Complexity	Low [32, 33]	High [32, 33]	Not estimated

Stiff systems offer rigid connections and reliable detumbling but require close proximity and have significant mass. NASA's bag capture system, which has an inflatable structure that forms a quasi-rigid connection, offers a balance by adapting to asteroid size uncertainties while enabling detumbling [15]. Based on these considerations, the NASA bag capture system was selected for its overall suitability for mission requirements.

- **Step 6:** Finally, the detumbling phase stabilizes the asteroid's rotation. The spacecraft fires its thrusters to counteract the asteroid's spin and reorient the combined asteroid–spacecraft assembly to a rest position, which ensures safe handling and transport during the return phase. For this purpose, it is assumed that the model has perfect knowledge of the asteroid's mass properties, considering it as a perfect sphere with uniform mass distribution. Therefore, similarly to the previously discussed model of matching the spin rate, an attitude control law is created. The method to obtain the propellant consumption given the torque command is identical to step 3. In reality, the mass properties of the asteroid are unknown. Therefore, this detumbling step should also involve some test maneuvers to estimate the inertia matrix of the asteroid, in order to adjust the control commands applied to the propulsion system.

Although simulators compute *TOF* and propellant consumption for each individual step, a constant duration of 120 days is assumed for the entire RPO phase to account for operational system checks with Earth-based control centers. This value is adopted from the NASA ARM feasibility study [15].

D. Spacecraft Sizing

The spacecraft sizing model determines a feasible total spacecraft mass for completing the asteroid capture mission. It relies on ΔV values throughout the mission and the *TOF* for each phase. These parameters are obtained from a full iteration of the trajectory model, ensuring alignment with mission requirements. This is achieved by allocating mass across each spacecraft subsystem.

In order to accomplish this task, NASA's Dynamic Rocket Equation Tool (DYREQT) is utilized, as it enables detailed sizing of a vehicle based on various mission and spacecraft specifications. DYREQT is built on top of OpenMDAO, an open-source Multidisciplinary Design Analysis and Optimization (MDAO) framework. OpenMDAO supports advanced features such as automatic differentiation, parallel computing, and gradient-based optimization [36]. By leveraging these capabilities, DYREQT can efficiently optimize spacecraft mass by examining trade-offs across the multiple subsystem models.

DYREQT's modeling process requires the decomposition of the asteroid capture mission into a specified "campaign." This campaign is composed of two distinct parts: the parametric mission definition and the vehicle (spacecraft) definition. These components will be discussed in detail individually, followed by an explanation of how they are implemented within the overall campaign structure.

1. Parametric Mission Definition

DYREQT requires that the mission be defined by one or more "branches", which are sequences of events representing distinct mission operations. All branches are anchored in simulated time by the first branch, so that any time passed during the simulated mission can be referenced to one specified epoch. The parametric mission definition endeavors to segment the asteroid capture mission into several sets of these branches, each consisting of interconnected events. The

result is a model of the mission such that, when the branches are considered as a whole, the entire mission is adequately modeled from initial departure burn to the storage orbit maneuvers. Figure 3 describes how the entire mission is defined within DYREQT, with each branch's specific series of events listed.

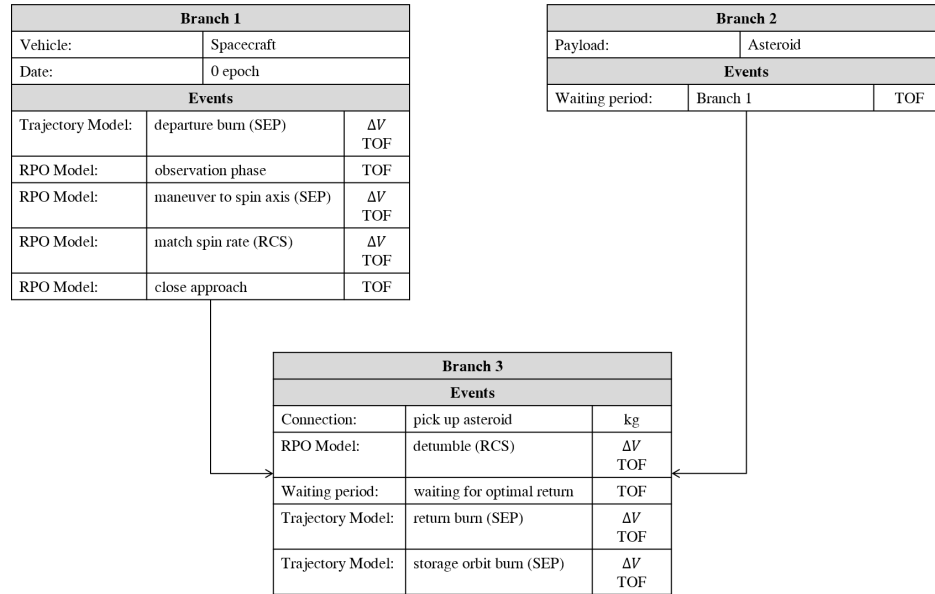


Fig. 3 Mission breakdown

With a clear understanding of the branch definition of the mission, each event within each branch can be further detailed.

Branch 1: Spacecraft Event Definition

- Trajectory Model departure burn - Defined by the continuous burn that the spacecraft needs to make to leave the initial Earth-orbit and rendezvous with the chosen asteroid
- RPO Model observation phase - Determines waiting period that needs to occur for the spacecraft to observe the asteroid and determine the asteroid' spin axis
- RPO Model maneuver to spin axis - The burn required to position the spacecraft along the spin axis of the asteroid
- RPO Model match spin rate - The RCS maneuver to rotate the spacecraft to match the asteroid's spin rate
- RPO close approach - The waiting time for the spacecraft to approach the asteroid

Branch 2: Asteroid Event Definition

- Waiting period Branch 1 - Waiting period of the asteroid, which includes the amount of time for branch 1 to complete its specific events

Branch 3: Branch Connection

- Connection pick up asteroid - Asteroid capture event
- RPO Model detumble - Maneuver to detumble and despin the asteroid, thus bringing it to a stable state
- Waiting period for optimal return - Waiting time of the spacecraft in asteroid's orbit in preparation for the return journey
- Trajectory Model return burn - The burn required for the spacecraft to return to cislunar space
- Trajectory Model storage orbit burn - The burn and *TOF* estimated to place the spacecraft-asteroid system into a stable DRO

2. Spacecraft Definition

DYREQT also requires that the vehicle within the campaign be defined explicitly. Detailed definition of the spacecraft allows for the allocation of mass across all subsystems during the sizing process, and enables the spacecraft to be run against the previously defined parametric mission.

The spacecraft is defined here by several "element groups", or systems, that comprise it, such as the propulsion system, fuel storage tanks, the power system, the thermal management system, avionics, attitude control systems, and the capture system. These element groups are further composed of sub-elements representative of various subsystems. These sub-element models can be physics-based, empirical, or externally defined. The vehicle's definition and decomposition are depicted graphically in Figure 4.

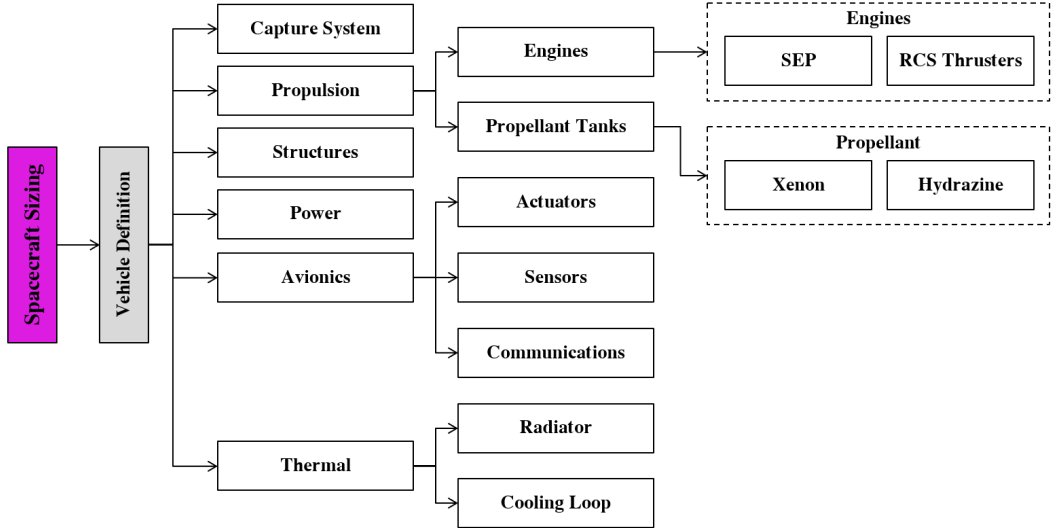


Fig. 4 Subsystem group architecture

One particular system of note is the Capture System, which is necessary to successfully capture the asteroid during mission operations. Because the capture system's properties are based on the asteroid of interest, the mass of the capture system is a fixed, calculable value. Thus, a capture system sizing model exists external to DYREQT, calculates the mass necessary for the capture system, and passes it to DYREQT as a fixed-mass, so that DYREQT does not alter this known, pre-sized component's properties.

The standalone capture system sizing model models a bag capture system, based on the NASA bag design, and estimates the total mass of the system based on the asteroid's diameter and the uncertainty in its measurement. This involves decomposing the capture system into its four main components and estimating their respective masses by considering assumed materials and scaling their volumes relative to the asteroid's size. An overview of the NASA bag capture system and its primary components is presented in Figure 5.

The first component, the inflatable exoskeleton, is assumed to be made from neoprene-coated Kevlar. This material choice is justified by its prior use in aerospace applications, notably in the inflatable structure of the Inflatable Antenna Experiment by the SPARTAN satellite and the inflatable aeroshell of NASA's Low-Density Supersonic Decelerator (LDSD) project [37]. The airbags, the second component, are similarly assumed to be made of neoprene-coated Kevlar, based on the same justification.

The third component is the structure of the robotic arms, for which carbon fiber is selected as the primary material. This selection is supported by its application in the ESA Smart Spacewalker, a robotic arm utilized on the International Space Station (ISS), offering a balance of strength and lightweight characteristics suitable for space operations.

Finally, the actuators of the robotic arms are modeled after the HT1 Rotary Incremental Actuator produced by Moog. This actuator was chosen as the lightest commercially available option capable of providing the maximum torque necessary to deploy the inflatable exoskeleton, taking into account the gravitational forces exerted by the Sun during deployment.

3. Implementation of the Campaign

With the vehicle and mission thoroughly defined, DYREQT can be utilized to perform its detailed sizing process. The spacecraft is run through all three branches of the mission, and mass is allocated to each individual component within the vehicle's definition. These masses also include built-in redundancy for uncertainty considerations. The

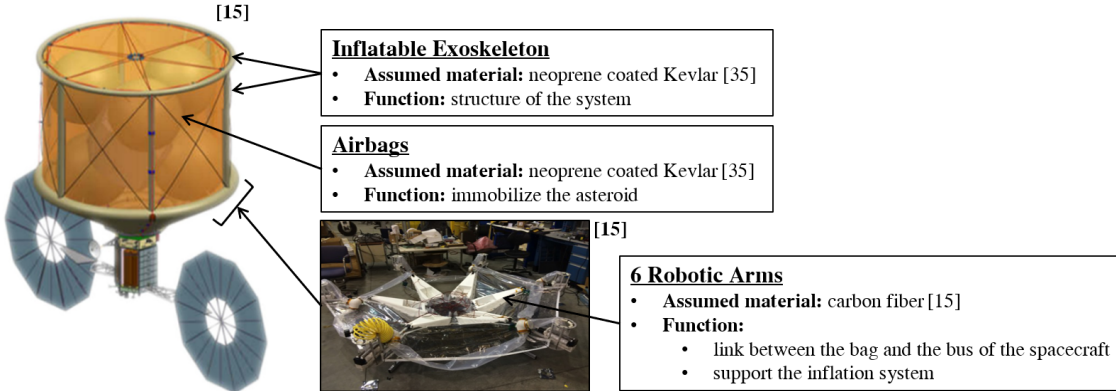


Fig. 5 NASA Bag capture system and main components

masses of these components can then be summed to find the spacecraft's total mass as an output of the DYREQT sizing process.

The total mass can then be compared to the trajectory model's initial mass estimate. If the masses are very close, iteration can stop, and the spacecraft is considered sized, with each subcomponent having an individually calculated mass. If the masses are not close, iteration is required, and the total mass from the DYREQT output can be passed back to the trajectory analysis model for further iteration. If the DYREQT output mass is larger than the maximum mass the launch vehicle can support, the spacecraft/mission design is considered infeasible.

IV. Results & Discussion

The framework described in the previous section is implemented using a combination of DOE and surrogate modeling techniques. These surrogate models enable rapid feasibility assessments and preliminary mission analyses for asteroid capture missions. This section presents the implementation process and case study results for two different NEAs, 2008 EA9 and 2009 BD, demonstrating the tool's capabilities.

A. Implementation using DOE, Surrogate Models and Dashboard

Mission and spacecraft designs depend on numerous variables, such as the launch window, mission duration constraints, propulsion system architecture, and uncertainties in asteroid parameters, resulting in an extremely large design space. Exhaustively simulating all possible combinations is computationally impractical. To address this, first, the project focuses on understanding the influence of timeline parameters and uncertainties in asteroid properties on an asteroid capture mission. Second, to efficiently explore this trade space while managing computational cost, a DOE approach is applied. A DOE is a systematic method for planning simulations or experiments to gain maximum information about the system with a limited number of runs. Based on the DOE results, surrogate models are constructed for key mission parameters, including the probability of mission feasibility, spacecraft gross mass, and mission duration. Surrogate models are simplified mathematical approximations that emulate the behavior of complex simulations, enabling rapid evaluation of outcomes across the design space. In this way, we can identify promising mission configurations, perform sensitivity analyses, and support robust early-phase decision-making without the computational burden of full-scale simulations. The DOE is constructed, using the tool JMP, with 200 cases for each NEA, balancing coverage of the design space with computational feasibility since a single simulation takes approximately one hour on a standard computer. The DOE included the following design variables:

- launch window
- mission window (i.e., the maximum allowable mission duration)
- asteroid mass
- asteroid mean diameter

Other parameters, such as the propulsion and capture systems, are held constant to isolate the effects of the selected variables and ensure a consistent exploration of the trade space. The ranges of these variables for the case study on the asteroids 2008 EA9 and 2009 BD are shown in Table 2. The variation of the asteroid mean diameter and mass allows

one to take into account the uncertainty on these parameters, while the mission window and the launch window serve as constraints for the M&S framework. The main outputs include:

- the mission duration for each mission phase with the associated ΔV
- the spacecraft gross mass with a subsystem-level breakdown
- the feasibility of the mission

Table 2 Ranges of the selected design variables

Parameters	Asteroid Mean Diameter (m)	Asteroid Mass (metric tons)	Mission Window (years)	Launch Window (years)
Ranges for 2008 EA9	7–20 [15]	65–260 [15]	5–20	2026–2031, 2031–2036
Ranges for 2009 BD	4–10 [15]	245–1180 [15]	5–20	2026–2031, 2031–2036

Using the results of the DOE, surrogate models are built with the JMP software. Two modeling approaches are employed: neural networks and response surface methods. To ensure the robustness of these models, the DOE dataset is divided into training and validation subsets, following a 80%–20% split. The surrogate models are evaluated against the following validation criteria:

- Coefficient of determination (R^2) greater than 0.8 for both training and validation datasets.
- Actual vs. Predicted plots showing no discernible patterns or clustering.
- Residual vs. Predicted plots with no visible trends or clusters, and residuals remaining within 10% of the minimum predicted value.

These criteria ensure that the models accurately capture the underlying behavior of the system while avoiding overfitting.

Finally, an interactive dashboard is developed to serve as an interface between the tool and the user. The dashboard allows selecting the target asteroid and visualizing the trade-off between different mission alternatives, as described in the following sections.

B. Case studies of the asteroids - 2008 EA9 and 2009 BD

After validating the M&S framework, case studies are made on the 2009 BD and 2008 EA9 asteroids. This subsection discusses their results, while demonstrating how a mission planner can explore the trade space of an asteroid capture mission.

1. Feasibility Analysis

The user can initially assess the feasibility of a mission based on the selected target NEA and the associated design variables. In this study, a mission is considered infeasible when either one of the following conditions is not satisfied:

- The computed mission duration exceeds the specified mission window.
- The computed spacecraft gross mass exceeds the maximum payload capacity of the selected launch vehicle.

Due to the limited number of cases evaluated, a Monte Carlo simulation is performed using surrogate models trained on the DOE dataset in JMP. This approach enables a probabilistic assessment of mission feasibility by accounting for uncertainty in key asteroid and mission parameters. The resulting feasibility contours, shown in Figures 6a and 6c for 2008 EA9, and Figures 6b and 6d for 2009 BD, illustrate the probability of a successful asteroid capture mission as a function of mission window and asteroid physical characteristics across two distinct launch windows. These plots allow users to explore how variations in asteroid mass and diameter affect mission feasibility across a broad design space.

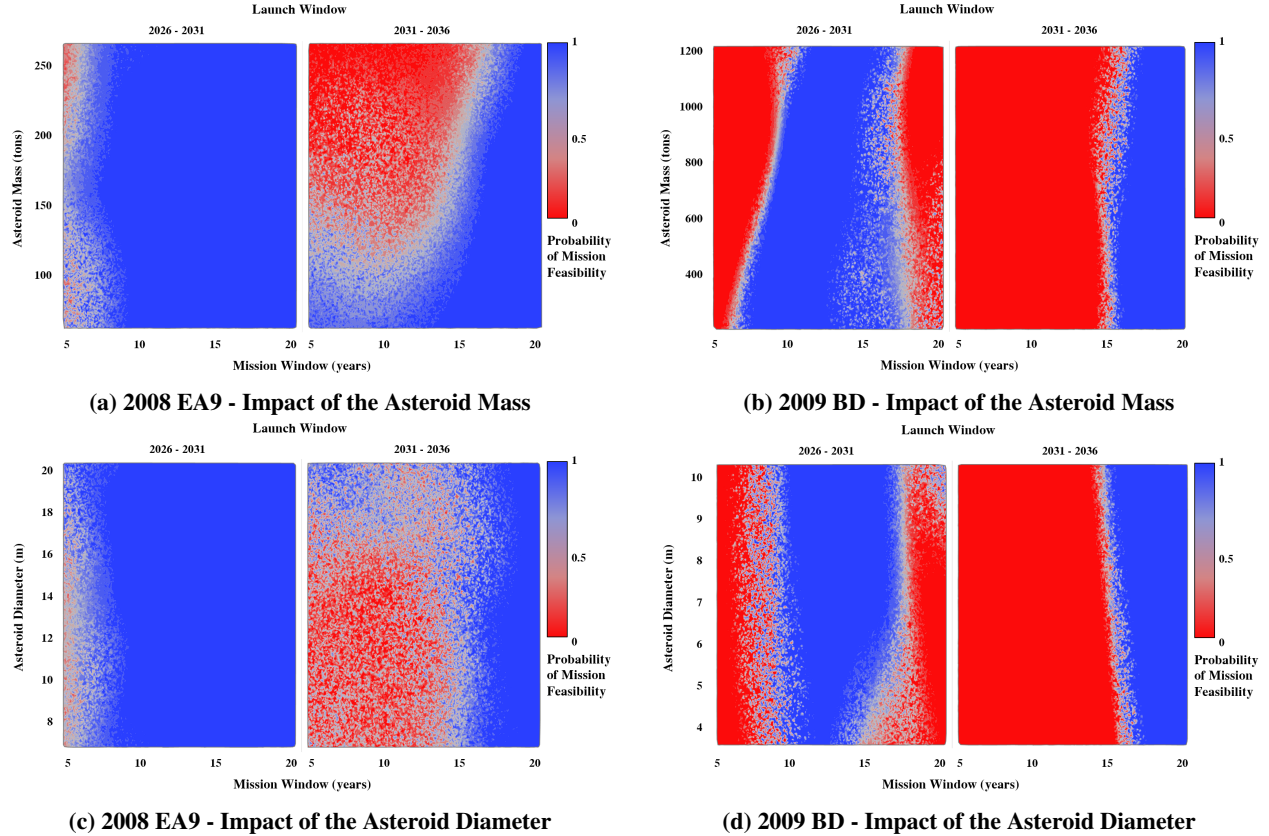


Fig. 6 Comparison of the Impact of Asteroid Mass and Diameter Uncertainties for 2008 EA9 and 2009 BD

In the contour plots, feasibility probability is represented by a color gradient: regions shaded in blue indicate higher feasibility, while those in red reflect lower feasibility. The vertical axis represents uncertainty in asteroid physical properties, mass for the upper plots and diameter for the lower plots. For asteroid mass, the uncertainty is modeled as a range from -50% to $+100\%$ relative to the nominal values reported in [15], reflecting the variability introduced by limited precision in ground-based observations. For asteroid diameter, the uncertainty range is directly adopted from the confidence intervals provided by the reference [15], which accounts for the observational limitations and resolution of the instruments used.

A key observation from both case studies is that the 2026–2031 launch window generally provides higher feasibility than the 2031–2036 window. This highlights the strong dependence of mission viability on planetary alignment and the relative orbital dynamics between Earth and the target asteroid. Additionally, the mission window itself emerges as a primary driver of feasibility, with most unfeasible cases resulting from mission durations exceeding the allowable timeframe.

Interestingly, the contour plots using asteroid mass and those using asteroid diameter as the vertical axis exhibit very similar feasibility trends. This indicates that, within the explored range, the physical properties of the asteroid, mass or diameter, have only a secondary influence on overall mission success.

Another important observation is that missions targeting 2009 BD are generally more constrained in terms of feasibility compared to those targeting 2008 EA9. As shown in Table 3, this is largely due to the differing orbital characteristics of the two asteroids. Specifically, 2009 BD has a higher semi-major axis and inclination, resulting in more energetically demanding transfer trajectories and a narrower design space for feasible missions, as shown in Figure 7.

However, the feasibility analysis of 2009 BD reveals a counterintuitive trend: missions with a window (maximum allowable duration) greater than approximately 17 years become infeasible, while windows between 9 and 17 years remain largely feasible. This result is unexpected, as a solution found for a shorter mission window should also be valid for a longer one, since the mission window defines the upper bound used in trajectory optimization. The inconsistency likely stems from numerical instabilities in the PyKEP optimization algorithm. When the mission window is excessively

large, the initial guess for the optimization may lie too far from a local optimum, causing the solver to fail to converge. Further work is underway to fix this issue.

Table 3 Orbital elements for selected asteroids and Earth [16]

Orbital Element	Earth	2008 EA9 $\pm \sigma$	2009 BD $\pm \sigma$
Eccentricity e	0.017	0.074 ± 0.001	0.0519 ± 0.000
Semi-major axis a [Astronomical Units (AU)]	0.999	1.049 ± 0.002	1.062 ± 0.000
Inclination i [degrees]	0.004	0.441 ± 0.006	1.267 ± 0.000
Longitude of ascending node Ω [degrees]	180.86	124.025 ± 1.578	253.158 ± 0.000
Argument of perihelion ω [degrees]	280.29	345.135 ± 3.360	316.656 ± 0.000
Time of perihelion passage t_P [Julian Date (JD)]	2025-January-1.8	2025-May-21.2 ± 3.7 days	2025-July-11.0 ± 0 days
Period P [years]	1.000	1.075 ± 0.002	1.095 ± 0.000

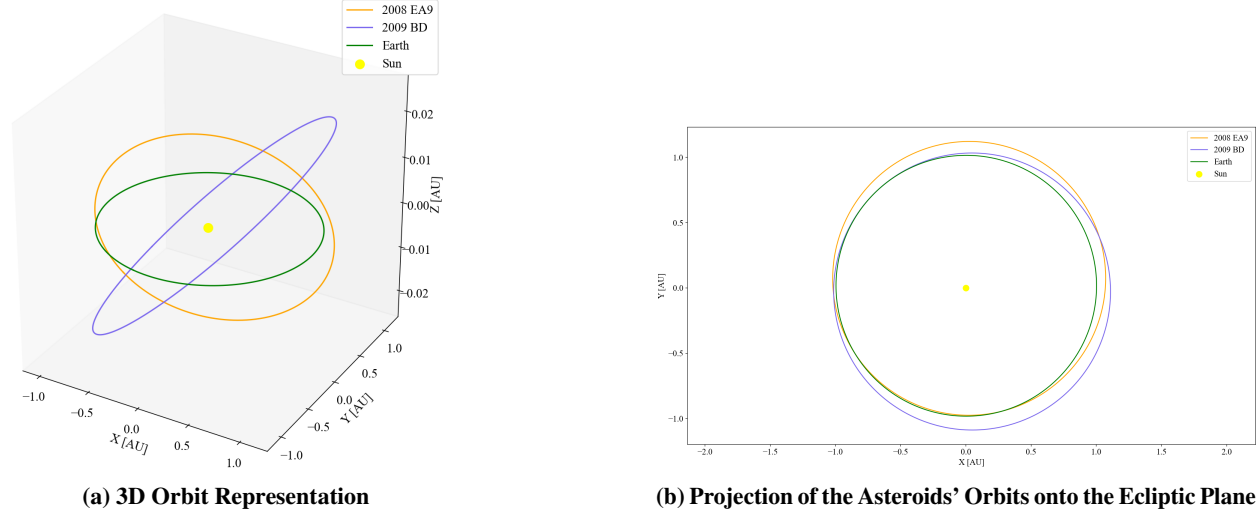


Fig. 7 Comparison of Orbits for Earth, 2008 EA9 and 2009 BD Asteroids

Through this analysis, users can evaluate the robustness of a mission concept under asteroid uncertainty and identify more promising mission configurations accordingly.

2. Preliminary Mission Analysis

Once the conditions for mission feasibility are met, the user can proceed with a preliminary mission analysis. This is facilitated by contour plots of asteroid parameters as functions of mission duration and spacecraft gross mass, as illustrated in Figures 8a–8d. The top figures have the color scale representing the uncertainty in asteroid mass, while the bottom figures have the color scale representing the uncertainty in asteroid diameter, which reflects the variability introduced by different ground-based observation methods and the associated limitations in measurement accuracy. As with the feasibility study, the contour plots are generated from Monte Carlo simulations based on surrogate models of spacecraft mass and mission duration. These plots highlight how uncertainties in asteroid properties propagate into key mission metrics, specifically, spacecraft mass and mission duration, which serve as critical indicators for mission evaluation and selection.

It is important to note that the design space is not fully populated across the entire range of mission durations and spacecraft masses. This is due to two factors. First, only cases with a mission feasibility probability greater than 0.5 are

retained from the Monte Carlo simulation. Second, since both spacecraft mass and mission duration are outputs of the surrogate models, varying the design variables does not guarantee complete coverage of the output space.

The results clearly demonstrate that higher asteroid mass tends to increase the required spacecraft mass, as the asteroid mass counts as the additional payload mass for the inbound phase. For instance, in the case of 2008 EA9, doubling the asteroid mass within its uncertainty bounds can lead to a 30–40% increase in spacecraft gross mass. Conversely, increasing the allowable mission duration can help reduce the spacecraft mass, offering a valuable trade-off in mission planning.

Similarly, the asteroid's diameter also influences spacecraft mass. This is evident in cases where the diameter reaches its upper threshold, yet the mission can still be accomplished with an 11-ton spacecraft (see Figure 8c). While diameter affects the design of the capture mechanism, and therefore contributes to total mass, it is not the dominant uncertain parameter driving spacecraft sizing or mission duration.

A comparison between the two case studies reveals that the most significant difference lies in the resulting spacecraft mass. This is consistent with the nominal mass of asteroid 2009 BD being approximately 4.5 times greater than that of 2008 EA9. However, the mission duration range remains comparable for both cases. Consequently, the trade-off between these two targets would be influenced primarily by mission-specific requirements, such as the desired amount of returned material, as well as the physical characteristics of each asteroid (e.g., composition, density, and structure).

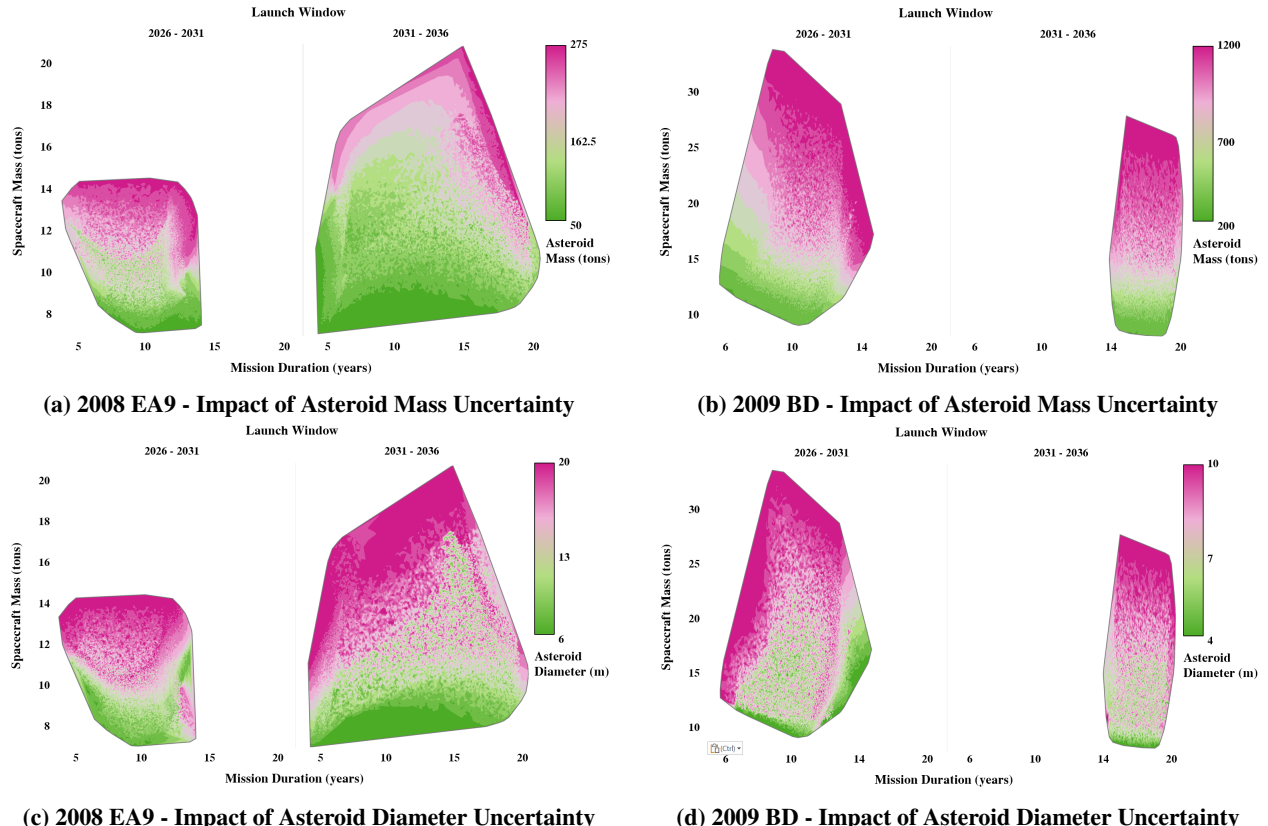


Fig. 8 Comparison of Contour Plots of Asteroid Mass and Diameter with Respect to Spacecraft Mass and Mission Duration

3. Mission Timeline and Spacecraft Sizing

A final tab, currently under development, will further support the preliminary mission analysis. When a user selects a point, or a specific combination of spacecraft mass and mission duration, on the contour plots presented in Figures 6 and 8, the tool will be able to display the detailed mission timeline, including the duration and the ΔV of each mission phase, as well as a subsystem-level mass breakdown of the spacecraft. The displayed information would correspond to the closest case in the DOE results relative to the selected point, based on proximity in spacecraft mass and mission

duration. These outputs are illustrated in Figures 9a and 9b.

This information provides a preliminary view of the spacecraft architecture and mission profile, offering critical insight during the conceptual design phase, where rapid evaluation of alternative concepts and early trade-offs is essential for guiding design decisions.

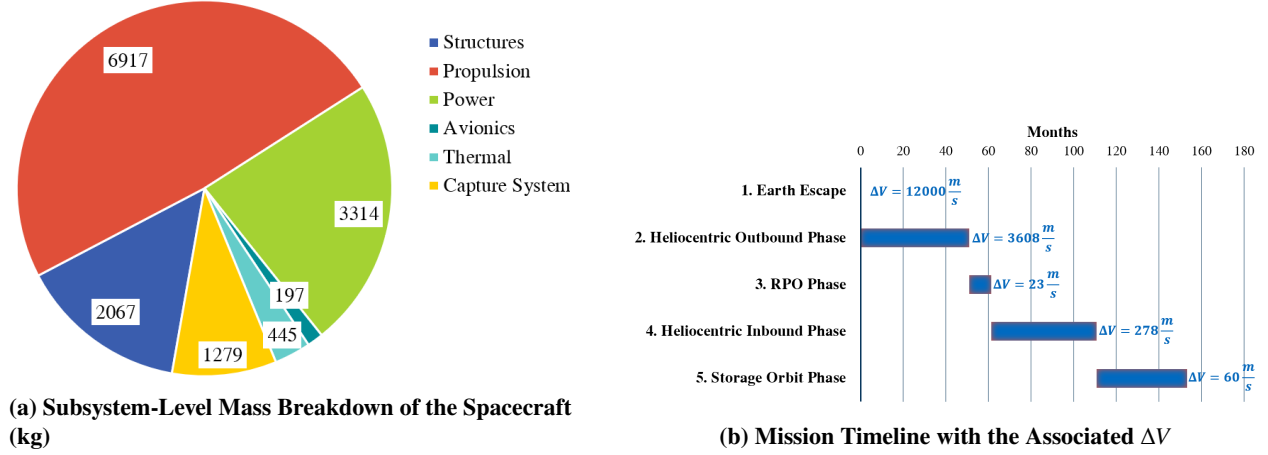


Fig. 9 Detailed mission and spacecraft designs displayed by the tool

V. Conclusion

This study developed a parametric tool to rapidly explore the design space of asteroid capture missions during the conceptual phase. The approach centered around the development of an integrated M&S framework that captures the three main pillars of this mission architecture: (1) low-thrust trajectory optimization using PyKEP, (2) modeling of RPO, and (3) subsystem-level spacecraft sizing based on trajectory and RPO outputs. A DOE was executed using this framework, and surrogate models were trained on the resulting dataset to enable rapid evaluation of mission feasibility and performance across a wide range of input parameters.

The tool supports early-phase decision-making by enabling systematic trade space exploration and visualization of key outputs such as spacecraft gross mass, mission duration, and feasibility. An interactive dashboard allows users to select a target asteroid and efficiently assess trade-offs between design variables. Key capabilities include visualizing the feasibility landscape, examining the impact of asteroid parameter uncertainties, and retrieving detailed outputs such as mission timelines and subsystem-level mass breakdowns for specific mission configurations.

Case studies conducted on two NEAs, 2008 EA9 and 2009 BD, highlight the sensitivity of mission design to the selected launch window and the benefits of extending mission duration in reducing spacecraft mass. These parameters are strongly correlated with mission cost, as mass is a principal driver of launch and system requirements. The impact of uncertainties in asteroid mass and diameter was clearly visualized. These uncertainties did not significantly affect mission feasibility, as the assumed launch vehicle (e.g., SLS with a 40-ton payload capacity) provided ample margin and was never exceeded by the computed spacecraft mass in any simulation. However, they did have a significant effect on spacecraft sizing.

The capabilities of the developed tool can be extended in several directions. First, future work could expand the analysis to a broader set of NEA targets with diverse sizes, compositions, and orbital characteristics. Second, the framework could be adapted to support other mission types, such as sample-return missions for larger asteroids or deflection/redirection missions for planetary defense scenarios. Additionally, future improvements to the M&S framework could include the incorporation of gravity assist maneuvers and alternative capture systems with their associated operational constraints, further enhancing realism and mission flexibility.

Acknowledgments

This project was supported and sponsored by the Georgia Institute of Technology Research Institute (GTRI). The team extends sincere thanks to Nicole Robertson and Paul Boyer for their invaluable guidance and constructive feedback

throughout the academic year. This work was made possible by the enthusiasm, collaboration, and support of everyone involved, all of whom are gratefully acknowledged.

Special thanks go to Alexandre Masset for his help and feedback on the RPO modeling; Jacob Z. Zhong, Sabina K. Maranto, and Jeffrey T. McNabb for their assistance with the Spacecraft Sizing Model, particularly with their knowledge of DYREQT; and finally, a warm thanks to John S. Robinson for his ongoing support and thoughtful feedback throughout the project.

References

- [1] Carter, J., “Will ‘Apophis’ Hit Earth In 2029? We’ll Know In 2027, Scientist Says,” , November 2024. URL <https://www.forbes.com/sites/jamiecartereurope/2024/11/06/will-apophis-hit-earth-in-2029-well-know-in-2027-scientist-says/>, accessed: 2025-05-07.
- [2] Jet Propulsion Laboratory, California Institute of Technology, “Sentry: Earth Impact Monitoring,” , 2025. URL <https://cneos.jpl.nasa.gov/sentry/>, accessed: 2025-05-07.
- [3] Lewis, J. S., *Mining the Sky: Untold Riches from the Asteroids, Comets, and Planets*, Helix Books, Addison-Wesley, Reading, Massachusetts, 1996.
- [4] NASA, “OSIRIS-REx In Depth,” , 2025. URL <https://science.nasa.gov/mission/osiris-rex/in-depth>, accessed: 2025-05-07.
- [5] Yoshikawa, M., Kawaguchi, J., Fujiwara, A., and Tsuchiyama, A., “The Hayabusa mission,” *Sample Return Missions*, edited by M. D. Fries, A. M. Nakamura-Messenger, and S. Siljeström, Elsevier, 2021, Chap. 6, pp. 123–143. <https://doi.org/10.1016/C2018-0-03374-5>.
- [6] NASA, “OSIRIS-REx Mission Overview,” , 2023. URL <https://science.nasa.gov/mission/osiris-rex/>, accessed: 2025-05-07.
- [7] McGuire, M. L., Strange, N. J., Burke, L. M., McCarty, S. L., Lantoine, G. B., Qu, M., Shen, H., Smith, D. A., and Vavrina, M. A., “Overview of the Mission Design Reference Trajectory for NASA’s Asteroid Redirect Robotic Mission,” *AAS/AIAA Space Flight Mechanics Meeting*, San Antonio, TX, USA, 2017, pp. 1–16. URL <https://ntrs.nasa.gov/citations/20170010282>.
- [8] Yuichi Tsuda, “Interview with Yuichi Tsuda on Hayabusa Mission,” , 2011. URL <https://web.archive.org/web/20110727084411/http://www.minorbody.org/yusejin/interview/interview04.html>, accessed: 2024-05-13.
- [9] Edwards, L., “Japanese space probe Hayabusa close to home,” , 2010. URL <https://phys.org/news/2010-06-japanese-space-probe-hayabusa-home.html>, accessed: 2025-05-13.
- [10] NASA, “NASA to Launch New Science Mission to Asteroid in 2016,” , 2011. URL <https://www.asteroidmission.org/?latest-news=nasa-to-launch-new-science-mission-to-asteroid-in-2016>, accessed: 2025-05-13.
- [11] Kerr, R. A., “NASA Aims to Grab Asteroid Dust,” , 2011. URL <https://web.archive.org/web/20110529114319/http://news.sciencemag.org/scienceinsider/2011/05/nasa-aims-to-grab-asteroid-dust.html>, accessed: 2025-05-13.
- [12] Wall, M., “NASA’s Asteroid-Capture Mission Explained (Infographic),” , 2013. URL <https://www.space.com/20612-nasa-asteroid-capture-mission-explained.html>, accessed: 2025-05-13.
- [13] Strange, N., Landau, D., McElrath, T., Lantoine, G., Lam, T., McGuire, M., Burke, L., Martini, M., and Dankanich, J., “Overview of Mission Design for NASA Asteroid Redirect Robotic Mission Concept,” *33rd International Electric Propulsion Conference*, Washington, D.C., USA, 2013, pp. 1–12. URL <https://ntrs.nasa.gov/citations/20150007879>.
- [14] Dave Doody, “Basics of Space Flight,” , 2022. URL <https://science.nasa.gov/learn/basics-of-space-flight/chapter7-1/#:~:text=Phase%20A%2C%20Preliminary%20Analysis,Phase%20E%2C%20Operations%20Phase>, accessed: 2025-05-13.
- [15] Muirhead, B. K., and Brophy, J. R., “Asteroid Redirect Robotic Mission Feasibility Study,” *2014 IEEE Aerospace Conference*, IEEE, Big Sky, MT, USA, 2014, pp. 1–14. <https://doi.org/10.1109/AERO.2014.6836358>.
- [16] Jet Propulsion Laboratory, California Institute of Technology, “JPL Small-Body Database Lookup Tool,” , 2025. URL https://ssd.jpl.nasa.gov/tools/sbdb_lookup.html#, accessed: 2025-05-07.
- [17] The International Astronomical Union Minor Planet Center, “The MPC Orbit (MPCORB) Database,” , 2025. URL <https://www.minorplanetcenter.net/iau/MPCORB.html>, accessed: 2025-05-07.
- [18] Irimies, D., “Solar Electric Propulsion,” , 2021. URL <https://www1.grc.nasa.gov/space/sep/>.
- [19] NASA, “True Blue: High-Power Propulsion for Gateway,” , 2023. URL <https://www.nasa.gov/image-article/true-blue-high-power-propulsion-for-gateway/>.
- [20] Kim, M., “Continuous Low-Thrust Trajectory Optimization: Techniques and Applications,” Ph.D. thesis, Virginia Polytechnic Institute and State University, Blacksburg, Virginia, Apr. 2005. URL <http://hdl.handle.net/10919/27046>, advisor: Dr. Christopher D. Hall.

- [21] Morante, D., Sanjurjo Rivo, M., and Soler, M., “A Survey on Low-Thrust Trajectory Optimization Approaches,” *Aerospace*, Vol. 8, No. 3, 2021, p. 88. <https://doi.org/10.3390/aerospace8030088>.
- [22] Bertrand, R., and Foliard, J., “Low-thrust Optimal Trajectories for Rendezvous with Near Earth Asteroids,” *18th International Symposium on Space Flight Dynamics*, ESA Special Publication, Vol. 548, edited by O. Montenbruck and B. Battick, European Space Agency, 2004, p. 481. URL https://www.issfd.org/ISSFD_2004/papers/P1028.pdf, bibliographic Code: 2004ESASP.548..481B.
- [23] SpaceX, “Falcon Heavy,” , 2024. URL <https://www.spacex.com/vehicles/falcon-heavy/>, [Online; accessed 15-October-2024].
- [24] EO Portal, “SLS (Space Launch System),” , 2024. URL <https://www.eoportal.org/other-space-activities/sls#sls-space-launch-system>, accessed: 2024-02-26.
- [25] Izzo, D., “PyGMO and PyKEP: Open Source Tools for Massively Parallel Optimization in Astrodynamics (The Case of Interplanetary Trajectory Optimization),” Technical Report ACT-RPR-MAD-2012-(ICATT), European Space Agency, Advanced Concepts Team, Noordwijk, The Netherlands, 2012. URL <https://www.esa.int/gsp/ACT/doc/MAD/pub/ACT-RPR-MAD-2012-%28ICATT%29PyKEP-PaGMO-SOCIS.pdf>.
- [26] Grilo, V. H. A., “Preliminary Trajectory Design of a CubeSat Mission to a Near-Earth Object,” Master’s thesis, Instituto Superior Técnico, University of Lisbon, Lisbon, Portugal, 2021. URL <https://fenix.tecnico.ulisboa.pt/downloadFile/1126295043838356/vasco-henrique-amaral-grilo-83739-thesis.pdf>.
- [27] Muirhead, B. K., and Brophy, J. R., “Asteroid Redirect Robotic Mission feasibility study,” *2014 IEEE Aerospace Conference*, IEEE, 2014, pp. 1–14. <https://doi.org/10.1109/AERO.2014.6836358>.
- [28] Kumar, Y., “Optimal Low Thrust Transfer for Relative Orbital Motion,” M. tech thesis, Indian Institute of Technology Kanpur, Kanpur, India, 2016. <https://doi.org/10.13140/RG.2.2.16899.91689>.
- [29] Markley, F. L., and Crassidis, J. L., *Fundamentals of Spacecraft Attitude Determination and Control*, Springer New York, New York, NY, 2014. <https://doi.org/10.1007/978-1-4939-0802-8>.
- [30] Pasand, M., Hassani, A., and Ghorbani, M., “A Study of Spacecraft Reaction Thruster Configurations for Attitude Control System,” *IEEE Aerospace and Electronic Systems Magazine*, Vol. 32, No. 7, 2017, pp. 22–39. <https://doi.org/10.1109/MAES.2017.160104>.
- [31] Barbee, B. W., Carpenter, J. R., Heatwole, S., Markley, F. L., Moreau, M., Naasz, B. J., and Van Eepoel, J., “Guidance and Navigation for Rendezvous and Proximity Operations with a Non-Cooperative Spacecraft at Geosynchronous Orbit,” *The Journal of the Astronautical Sciences*, Vol. 58, No. 3, 2011, pp. 389–408. <https://doi.org/10.1007/BF03321176>.
- [32] Shan, M., Guo, J., and Gill, E., “Review and Comparison of Active Space Debris Capturing and Removal Methods,” *Progress in Aerospace Sciences*, Vol. 80, 2016, pp. 18–32. <https://doi.org/10.1016/j.paerosci.2015.11.001>.
- [33] Poozhiyil, M., Nair, M. H., Rai, M. C., Hall, A., Meringolo, C., Shilton, M., Kay, S., Forte, D., Sweeting, M., Antoniou, N., and Irwin, V., “Active Debris Removal: A Review and Case Study on LEOPARD Phase 0-A Mission,” *Advances in Space Research*, Vol. 72, No. 6, 2023, pp. 3386–3413. <https://doi.org/10.1016/j.asr.2023.06.015>.
- [34] Gates, M., Mazanek, D., Muirhead, B., Stich, S., Naasz, B., Chodas, P., McDonald, M., and Reuter, J., “NASA’s Asteroid Redirect Mission concept development summary,” *2015 IEEE Aerospace Conference*, IEEE, 2015, pp. 1–13. <https://doi.org/10.1109/AERO.2015.7119163>.
- [35] Shan, M., and Shi, L., “Velocity-Based Detumbling Strategy for a Post-Capture Tethered Net System,” *Advances in Space Research*, Vol. 70, No. 5, 2022, pp. 1336–1350. <https://doi.org/10.1016/j.asr.2022.06.012>.
- [36] Gray, J. S., Hwang, J. T., Martins, J. R. R. A., Moore, K. T., and Naylor, B. A., “OpenMDAO: An open-source framework for multidisciplinary design, analysis, and optimization,” *Structural and Multidisciplinary Optimization*, Vol. 59, No. 4, 2019, pp. 1075–1104. <https://doi.org/10.1007/s00158-019-02211-z>.
- [37] Litteken, D. A., “Inflatable technology: using flexible materials to make large structures,” *Electroactive Polymer Actuators and Devices (EAPAD) XXI*, Vol. 10966, edited by Y. Bar-Cohen and I. A. Anderson, SPIE, 2019, pp. 1–10. <https://doi.org/10.1117/12.2500091>.